



REDUCTION OF TURBULENT NOISE FROM BACKWARD CURVED CENTRIFUGAL FAN WITH RECTANGULAR CASING

Hidechito HAYASHI¹, Seiji SHIRAHAMA², Ippei ODA²,
Tetsuya OKUMURA¹, Hiromitsu HAMAKAWA³

¹ *Nagasaki University, Mechanical Engineering, 1-14 Bunkyo machi,
Nagasaki, Japan*

² *Panasonic Ecology Systems Co., Ltd., R&D center, 4017 takakicho
Kasugai, Japan*

³ *Ooita University, mechanical engineering, 700 Tannohara Ooita, Japan*

SUMMARY

The backward-curved centrifugal fan with rectangular casing is investigated in relating to the turbulent noise. The acoustic transparent wall is used to find out the noise source. The turbulent noise consists of the different noise sources. The low frequency noise is generated from the impeller, the higher frequency range noise is generated from the casing wall. One of the side walls is the most important to the high frequency noise. The swirl flow near the shroud causes the large turbulence and generates the high frequency and large turbulent noise. We proposed the obstacle near the upper part of the side wall. It can reduced the noise level.

INTRODUCTION

The backward-curved centrifugal fan is obtained relatively high efficiency and low noise. The small size of this type fan is used in the air conditioner and air cleaner. In the recent application, the fan is not used the scroll casing but the rectangular casing, because of the compact size and flexible design.

The backward-curved centrifugal fans have been studied almost the case with the scroll casing⁽¹⁾⁻⁽⁴⁾. The flow characteristics is researched to improve the fan performance^{(1),(2),(4)} that is mainly concerned to the interaction between the tongue and the impeller^{(3),(5)}. The various geometries of the impeller and shroud are examined in the performance with experiments⁽⁶⁾. For the case of the air conditioner, there are studies in concerned to the interaction between the impeller and the heat exchanger⁽⁷⁾⁻⁽⁹⁾. In the case, the air from the fan flows in all directions.

In this paper, It is investigated the characteristics of the turbulent noise and its noise source at the rectangular casing by experiments and numerical simulation. The turbulent noise is analyzed by dividing the frequency range. Finally we proposed the obstacle near the upper part of the side wall. It can be reduced the noise level.

EXPERIMENTS AND SIMULATION METHODS

Experimental Apparatus

The performance of the test fan is measured with the wind tunnel as shown in figure 1. The test fan is set at the outlet of the semi-anechoic chamber. The flow rate is varied with the auxiliary fan and measured by the orifice. The pressure rise is obtained by the pressure difference between the chamber and atmosphere. The sound pressure level is measured by the 1/2 microphone at the 1m upstream from the bell-mouth in the semi-anechoic chamber. The sound signal is analyzed by the FFT analyzer.

The schematics of the test fan are shown in figure 2. The impeller is shown in figure 2(a). The inner and outer diameters are 142 and 230 mm. The span at the outlet is 60.5 mm. The number of blades is 7 and the blade geometry is two dimensional that is made with the thin plate, 1 mm thickness. The section geometry of the casing is shown in figure 2(b). The depth, width and height of the rectangular casing are 350, 350 and 158 mm, respectively. The impeller is set at the center of casing. The outlet section of the casing is 350*158 mm. It is so large to bare the whole impeller from the downstream. The fan with the scroll casing is examined to compare the performance, as shown in figure 3(a) and (b).

Figure 3(a) and (b) show the casing geometry. Figure 3(a) is the rectangular casing, it is called RC. The geometry is two dimensional. The impeller is set at the center of the casing. The distance between the impeller at the casing is 60 mm. Figure 3(b) is the scroll casing, it is called SC. The volute angle is 6 degree. The span is same to the rectangular casing. The acoustic transparent wall is

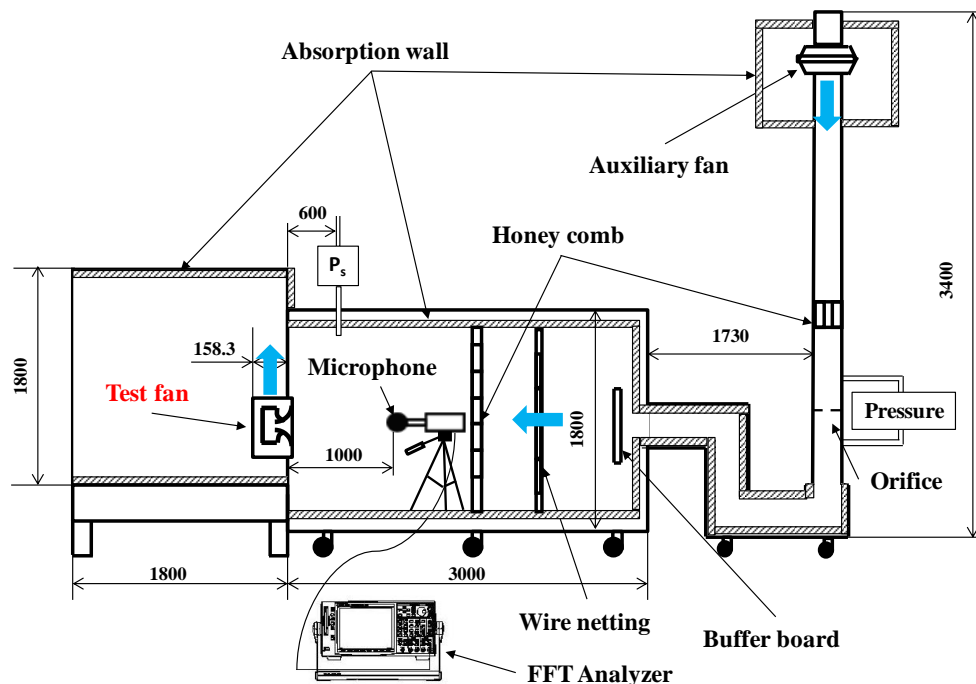


Figure 1 : Experimental apparatus

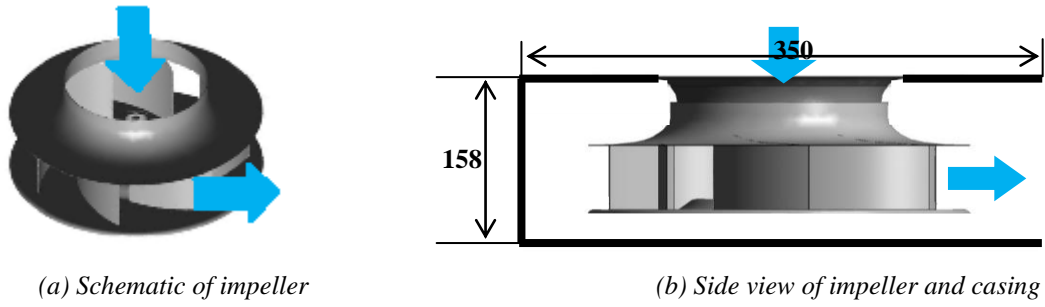


Figure 2 : Impeller and casing

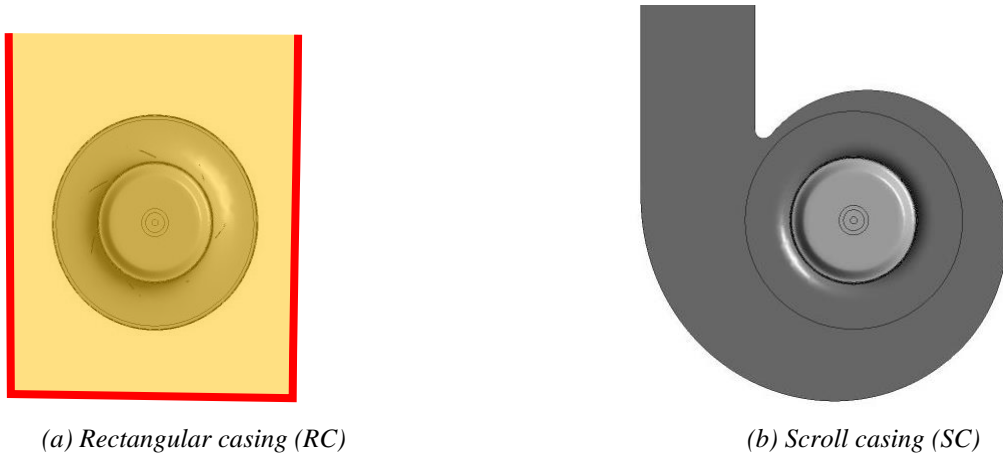


Figure 3 :Casing geometries

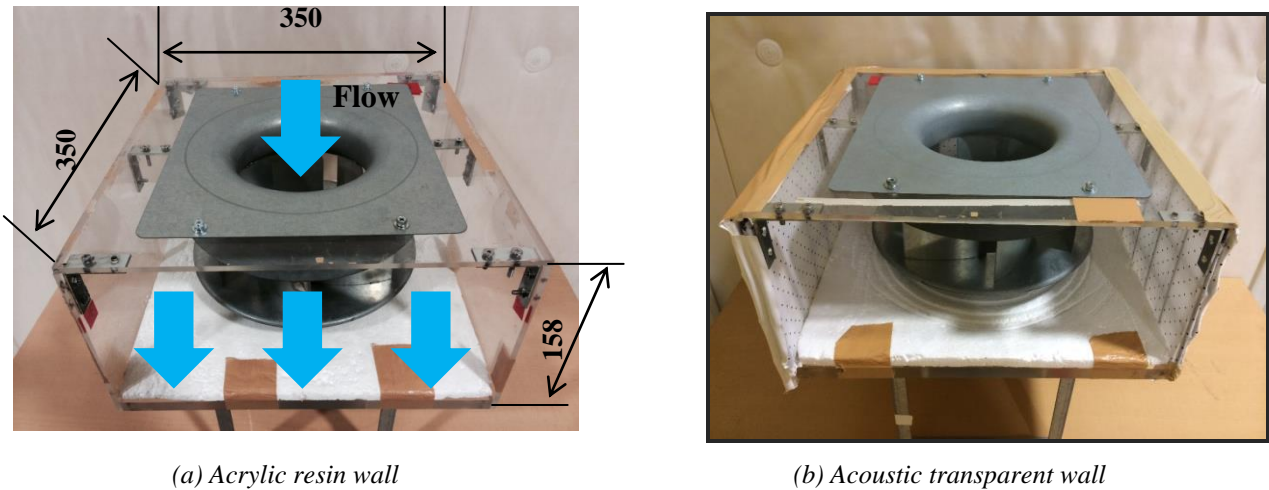


Figure 4 :Casing condition

used to make clear the sound source on the wall. The acoustic transparent wall passes through the acoustic pressure, but does not pass the flow. The dipole sound source does not generate on the acoustic transparent wall surface. Figure 4(a) and (b) show the casing geometries. Figure 4(a) is the original wall is made with acrylic resin. Figure 4(b) is the wall replaced to the acoustic transparent walls. Each side wall is replaced to the acoustic transparent wall.

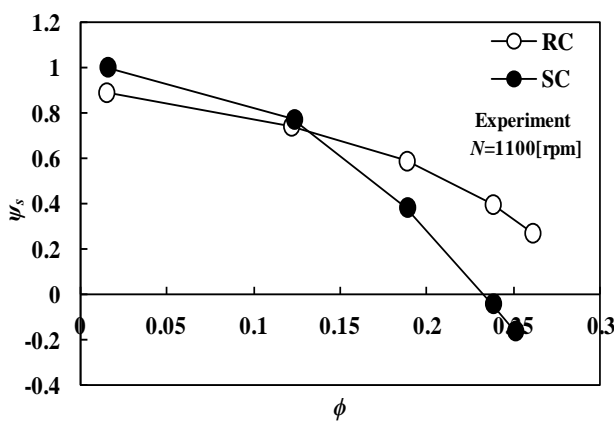
Simulation Condition

The numerical simulation is made by the commercial code ANSYS CFX 14.5. The main simulation condition is shown in table 1. Unsteady flow simulation is done that it is concerned to the

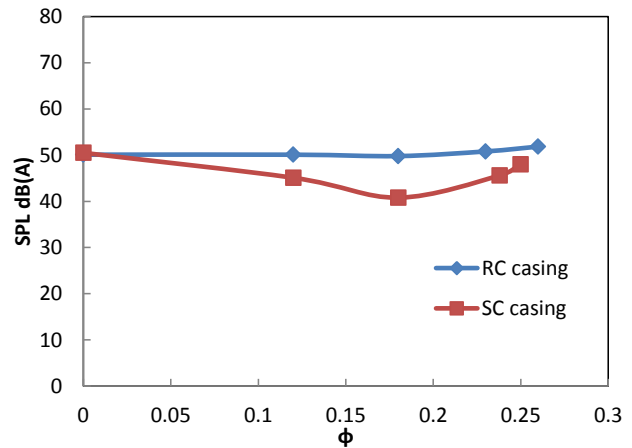
interaction between the rotating impeller and the casing. The rotating speed is 1100 rpm. The domain of the impeller is only rotating and the frozen rotor condition is set at the interface. The inlet boundary condition is set at atmospheric pressure that makes easy to calculate the pressure rise at the fan. The outlet boundary condition is set the mass flow rate. The turbulent model is SST. The time step is 0.106 msec. The iteration number is 3072. The last 2000 iterations are used to analyze the flow characteristics. The characteristics of the performance are obtained by the averaged data of unsteady simulation.

Table 1 : Simulation condition

Flow condition	Unsteady flow
Inlet boundary condition	Atmospheric pressure
Outlet boundary condition	Mass flow rate
Rotating speed	1100 rpm
Turbulent model	SST
Time step	0.106 msec
Iteration number	3072 (6 revolutions)



(a) Variation of static pressure coefficient



(b) Variation of SPL (A)

Figure 5 : Comparison of performances with casing geometry

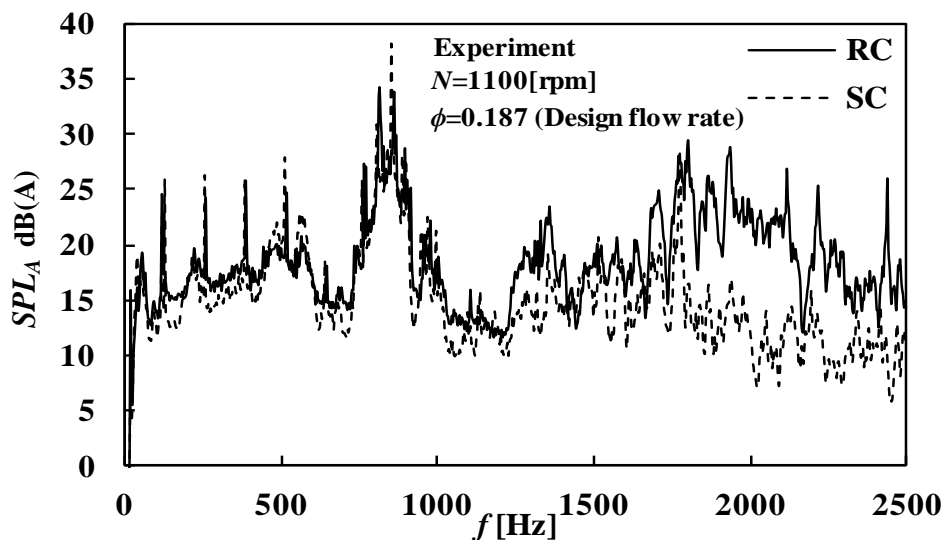


Figure 6 : Narrow band spectrum distribution of noise level (A-weighted)

RESULTS AND DISCUSSIONS

Fluid Performance and Noise Characteristics

The performance curves are shown in figure 5. This figure is compared to the different casings, the rectangular casing (RC) and scroll casing (SC). The pressure coefficient in figure 5(a) is gradually decreased with the flow coefficient in both casings.

The variation of the pressure coefficient with the flow rate is small at the rectangular casing compared with at the scroll casing. So the pressure of RC fan is high at the large flow coefficient. The fluid performance with RC fan is good compared with the SC fan at large flow rates. It indicates that the RC fan gives the good performance with compact and small size. The noise levels are shown in figure 5(b). The noise level of SC fan is gradually decreased with the flow coefficient up to design point (0.186). The noise level of RC fan is almost constant. The difference between these noise levels is about 10 dB near the design point. The turbulent noise of RC fan does not decreased at the design point.

Figure 6 shows the spectral distributions of RC fan and SC fan. It can be seen that there exist the discrete frequency noises under the 700 Hz that are caused by the interaction between the impeller and the casing. Especially the discrete frequency noise of SC fan is large that is caused by the interaction between the impeller and the tongue of casing. The discrete frequency noise of RC fan is small⁽¹⁰⁾. The broadband noise of RC fan is very large compared to SC fan. Especially the high frequency noise is very large. The difference of overall sound level in figure 5(b) is mainly caused by the frequency range over 1700 Hz.

Flow Characteristics

Figure 7(a) and (b) show that the time averaged velocity vectors. Figure 7(a) is the case of rectangular casing. At the RC fan, the upper wall, back wall and lower wall are named wall 1, wall 2 and wall 3. The velocity distribution in the casing is varied in circumferential location. There exist the large velocities near the wall 1 where the outflow from the impeller gathers to this region. The velocity near the wall 2 is small because of the high pressure and low flow rate at the location. Near the wall 3, the air out of impeller flows toward and strikes to the wall. Then the air bifurcates at the casing wall to backward and the exit of fan. At the case of SC fan, the air out of the impeller flows along the scroll casing in figure 7(b).

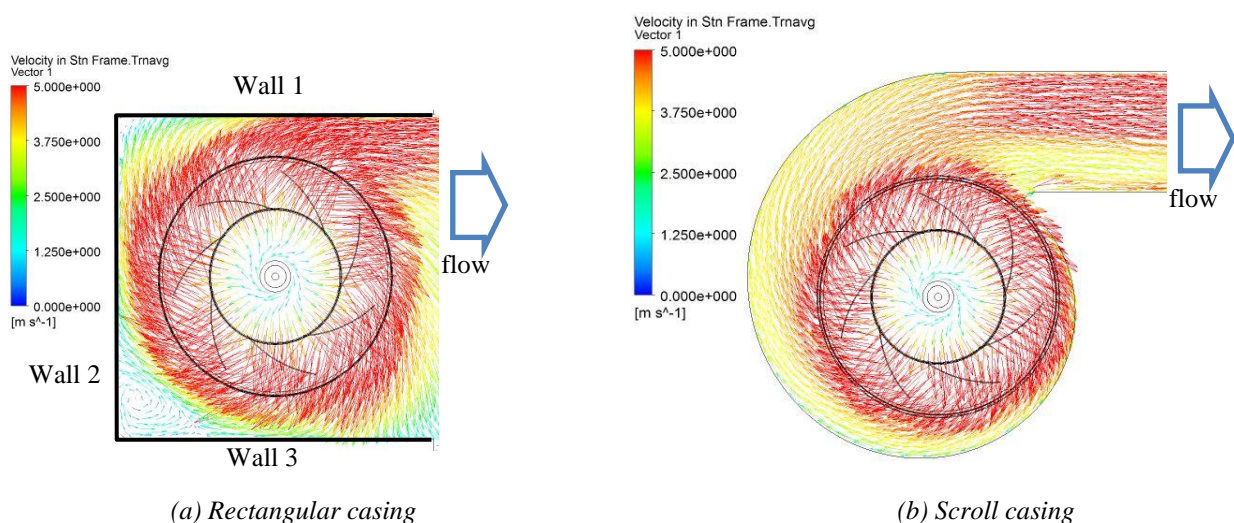


Figure 7 : Time averaged velocity vector distributions

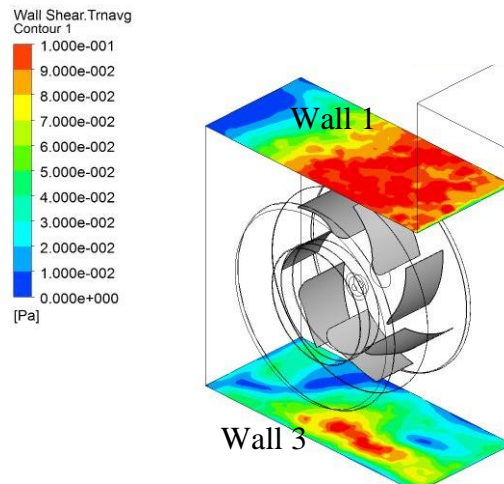
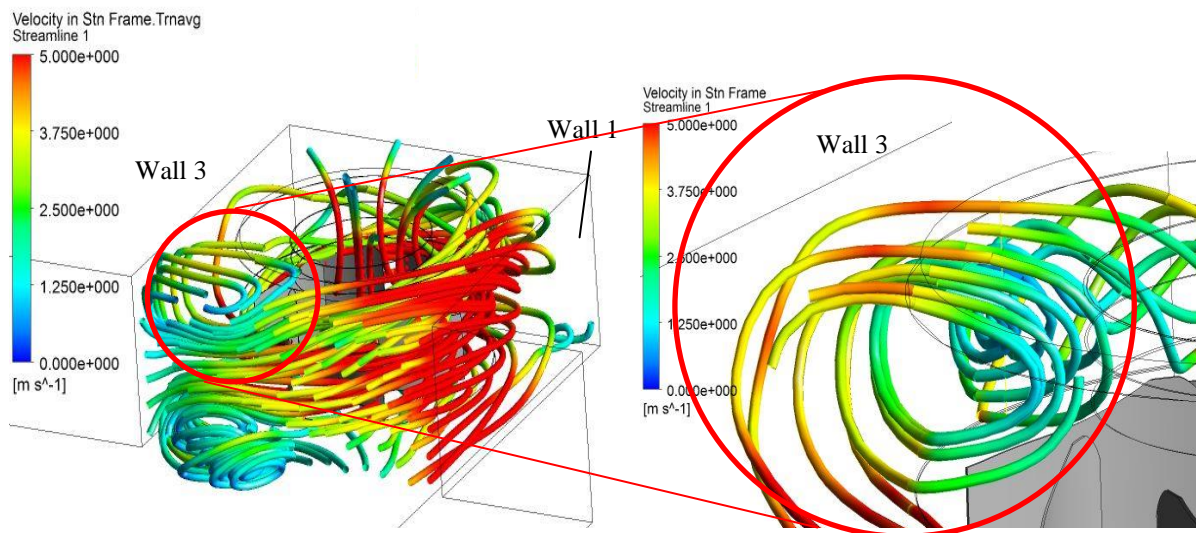


Figure 8 : Contour map of wall shear of casing wall



(a) In fan casing

(b) Over shroud near the wall 3

Figure 9 : Stream lines in the RC

Figure 8 shows the wall shear distributions on the side casings, wall 1 and wall 3. On the wall 1, there exists the strong shears at the outflow part on the wall1 that is corresponding to the velocities as shown in figure 7(a). On the wall 3, the strong shear exists at the upper side. This location is near the strike flow to the wall.

Figure 9 shows the stream lines in the casing. In figure 9(a), it can be seen the large velocity distribution in all pan near the wall 1 that the flow from the back and side part of the fan gathered. Near the wall 3, the stream lines strike to the wall 3 and turn to the upper part. The stream lines rolls up and goes back in the casing region. This flow makes the strong shear on the wall 3 in figure8. The detail of the shroud flow near the wall 3 is shown in figure 9(b). It is clear the swirl flow that the flow is unstable caused by the interaction between the back flow and the out flow from the impeller. This swirl flow generates the large turbulent noise.

Sound Characteristics

Figure 10 shows the estimated frequencies of Aeolian tones by Fukano's equation. The wake width and the relative velocities obtained from the simulation results as shown in figure 10(a). The

frequency 50 – 700 Hz of the Aeolian tone is generated from the impeller. The frequency varies very large in circumference locations. As shown in figure 10(a), the flow in the impeller is varied in

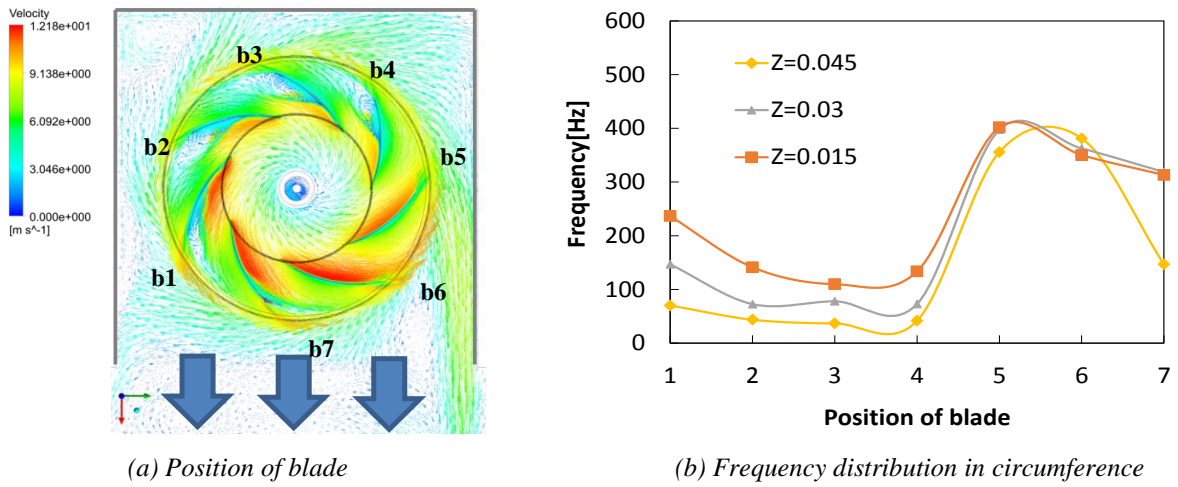


Figure 10 :Estimated frequency of turbulent noise

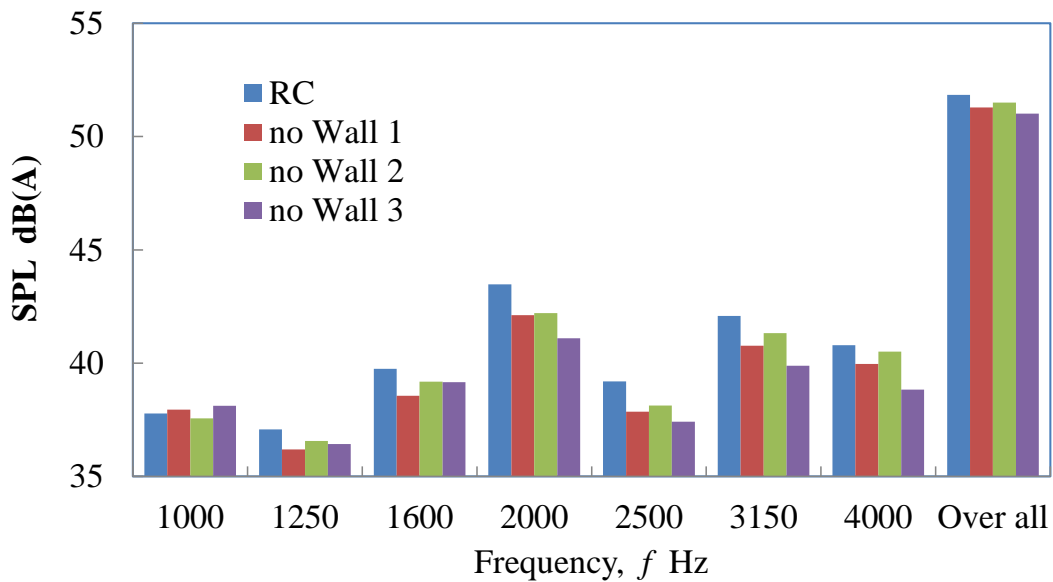


Figure 11 :1/3octave distribution at each wall removed

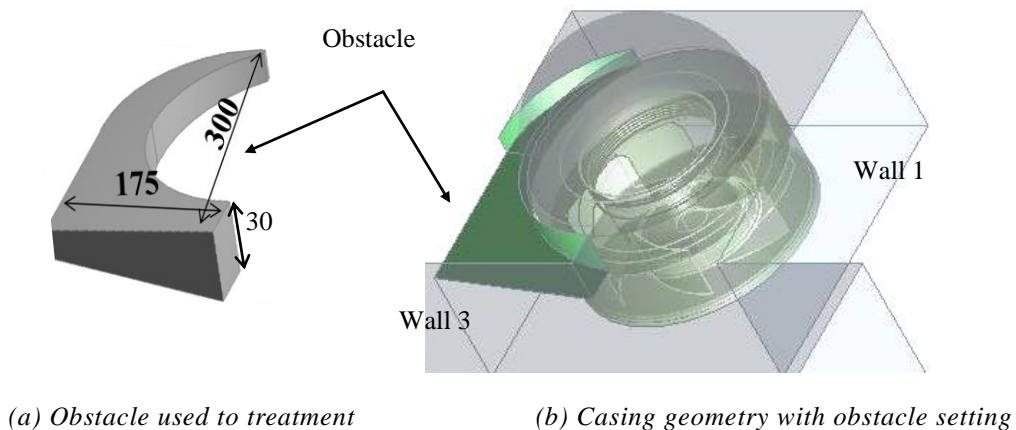


Figure 12 – Treatment of rectangular casing

circumference. The large flow separation occurs at b1 to b3 and the wake width becomes large. But the flow attached on the blade at b5 to b6 and the wake width becomes small. The level of the Aeolian tone is 56.2 dB by Fukano's equation that is equal to the experimental result at the design point. This shows the turbulent noise of low frequencies is mainly caused by the blades of impeller.

Figure 11 shows the 1/3 octave distributions for each acoustic transparent wall. The condition of no Wall 1 is that the side wall 1 of casing is changed from rigid wall to the acoustic transparent wall that reduces the dipole sound generated from the wall. When the side wall is changed to the acoustic transparent wall, the SPLs over 2000 Hz are reduced in all frequencies. This indicates that the noise at high frequencies is mainly caused from the side walls. Especially the reduction of sound level is large at the no Wall 3.

Sound Reduction with Obstacle

We propose the treatment with the obstacle to prevent this strong swirl flow and back flow near the shroud. Figure 12 shows the obstacle. Figure 12(a) is the obstacle that the width is a half of the casing width. The arc geometry is corresponding to the outer diameter of the impeller. The height is kept in the upper shroud region that does not prevent the out flow from the impeller. The setting condition is shown in figure 12(b). The thickness is 30 mm at the front and gradually thinned to the

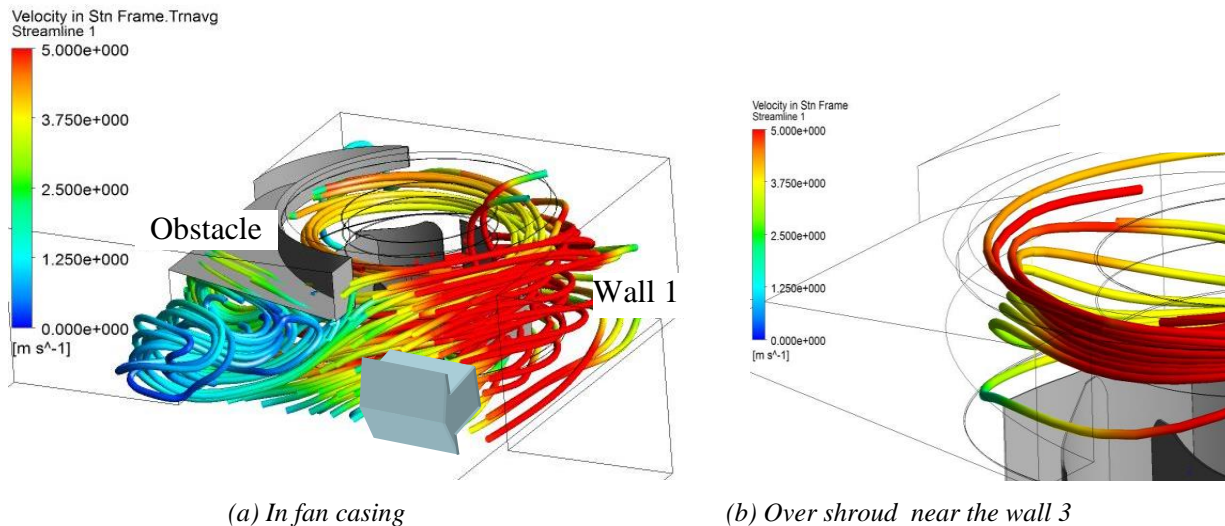


Figure 13 : Stream lines in the RC with obstacle

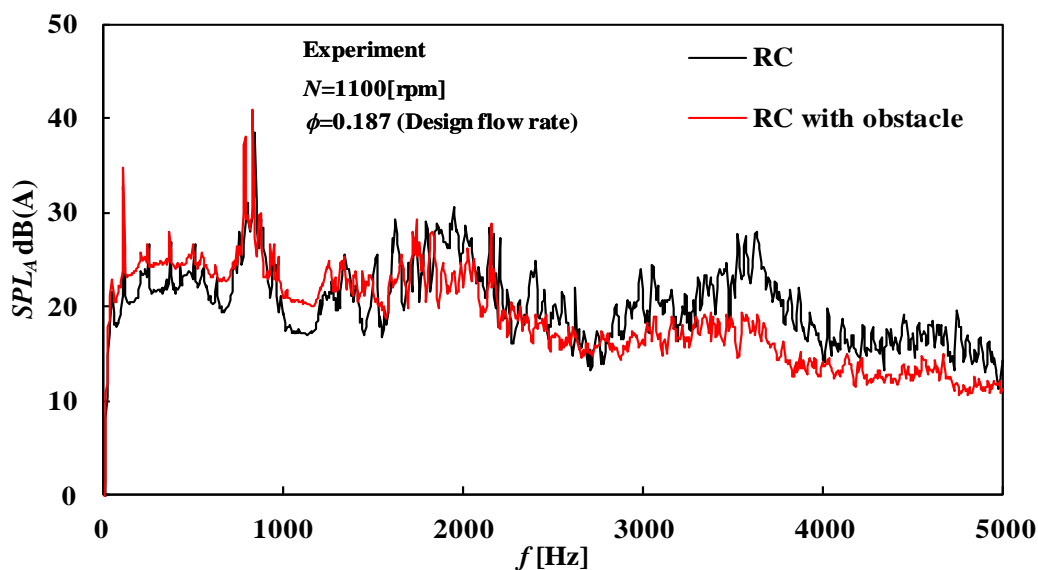


Figure 14 : Spectrum distribution of the SPL with and without obstacle

backward direction. Figure 13 shows the streamlines with the obstacle. In figure 13(a), there also exists the large velocity near outlet on the wall 1. The main outflow from the fan is similar to the no obstacle. Near the wall 3, the flow direction is not to the back-ward, but to the outer-ward of the fan. So there does not exist the swirl flow in figure 13(b). So this obstacle can prevent the swirl flow near the wall 3.

Figure 14 shows the spectrum distributions of SPL with the obstacle and without it. The distribution of the casing with obstacle is lower than the case of no treatment near the 2000 Hz and over 2700 Hz. The obstacle at the upper part in the casing indicates the reduction of the high frequency noise.

Figure 15 is the integrated sound energy for each frequency range. At the low frequency range, the sound power is a little increased, but at the middle and high frequency range the noise level is reduced very much. Especially at the high frequency range the reduction of noise level about 5 dB reduced. So the total SPL can be reduced.

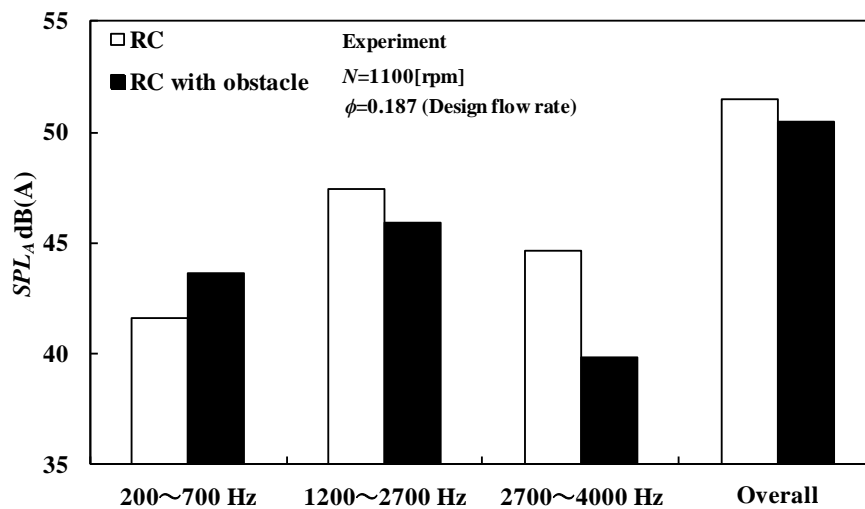


Figure 15 – Partial SPL with and without obstacle

CONCLUSIONS

The backward-curved centrifugal fan with rectangular casing is used in relating to the turbulent noise. The following results are obtained.

1. The turbulent noise consists from the low frequency and the high frequency ranges that are caused by the different noise source less than 800 Hz and over 1700 Hz.
2. The low frequency noise is generated from the impeller and the high frequency noise is mainly generated from the casing wall.
3. The wall 3 influences the high frequency turbulent noise very much.
4. We proposed the obstacle to reduce the high frequency noise and the noise level of high frequency is reduced about 5 dB.

REFERENCES

- [1] Y. Yokoi, S. Inagaki – *Experimental Study of Flow Feature in Spiral Casing of Turbo Fan*, Turbo Machinery, Vol.33-4, pp241- 249, **2005**
- [2] D Qi , Y Zhang, S Wen, and Q Liu – *Measurement and analysis of three-dimensional flow in a centrifugal fan volute with large volute width and rectangular cross-section*, IMechE, Vol. 220, pp.133-153, **2006**
- [3] Yamazaki, S. Komatsu, T. Obata, S. Yokoyama – *Investigation of Flow Pattern in a Backward-Curved Fan and Influence of Its Fan Shape on the Performance and Noise*, JSME, Vol.65-636, pp.2770-2776, **1999**
- [4] Yu, S. Li, W. He, W. Wang, D. Huang, Z. Zhu – *Numerical Simulation of Flow Field for a Whole Centrifugal Fan and Analysis of the Effects of Blade Inlet Angle and Impeller Gap*, HVAC&R Research, Vol.11-2, pp.263-283, **2005**
- [5] W. H. Jeona, D. J. Leeb – *A numerical study on the flow and sound fields of centrifugal impeller located near a wedge*, J. Sound and Vibration, Vol.266, pp.785-804, **2003**
- [6] A. Behzadmehr, J.B. Piaud, R. Oddo, Y. Mercadier – *Aero-Acoustical Effects of Some Parameters of a Backward-Curved Centrifugal Fan Using*, DoE, Vol.12-2, pp.353-365, **2006**
- [7] S. Yamashita – *Silent and Super Link System of Ceiling Recessed Type Packaged Air Conditioner*, Refrigeration, Vol.67-776, pp.622-627, **1992**
- [8] T. Mochizuki, T. Nimura, I. Moriyama, H. Kogure, Y. Aizawa, S. Nishikawa – *A New cassette Type Air Conditioner with 4-way Adjustable Auto Flaps*, Refrigeration, Vol.67-776, pp.600-607, **1992**
- [9] Y. Kodama, H. Hayashi, T. Sanagi, K. Kinoshita – *Noise Generated by a Centrifugal Fan without Scroll Casing (Effects of the distance between the leading edge of the blades and the wall of the mouthpiece, the geometry at the outlet of the bell-mouth and the gap of the mouthpiece)*, JSME, Vol.63-613, pp3025-3032, **1997**
- [10] H. Hayashi, K. Nakamura, S. Sasaki, S. Shirahama, A. Nagata, *Flow Characteristics of Turbo Fan with Rectangular Casing*, Turbo Machinery, Vol.39-10, pp624-631, **2011**

NOMENCLATURE

f	Frequency	Hz
N	Rotating speed	rpm
z	Span-wise position	m
ϕ	Flow coefficient	
ψ	Pressure coefficient	